

Spontaneous and triggered vortices in polariton OPO superfluids

F. M. Marchetti,¹ M. H. Szymańska,² C. Tejedor,¹ and D. M. Whittaker³

¹*Departamento de Física Teórica de la Materia Condensada,
Universidad Autónoma de Madrid, Madrid 28049, Spain*

²*Department of Physics, University of Warwick, Coventry, CV4 7AL, UK**

³*Department of Physics and Astronomy, University of Sheffield, Sheffield, S3 7RH, UK
(Dated: March 25, 2010)*

We study non-equilibrium polariton superfluids in the optical parametric oscillator (OPO) regime using a two-component Gross-Pitaevskii equation with pumping and decay. We identify a regime above OPO threshold, where the system undergoes spontaneous symmetry breaking and is unstable towards vortex formation without any driving rotation. Stable vortex solutions differ from metastable ones; the latter can persist in OPO superfluids but can only be triggered externally. Both spontaneous and triggered vortices are characterised by a generalised healing length, specified by the OPO parameters only.

PACS numbers: 42.65.Yj, 47.32.-y, 71.36.+c

Since the first observation of stimulated scattering [1], resonantly driven polariton microcavities have been the subject of intensive research. Significant advances have taken place towards a new generation of low threshold lasers and ultrafast optical amplifiers and switches. However, only very recently resonantly pumped polaritons have been shown to exhibit a new form of non-equilibrium superfluid behaviour [2–4]. In the OPO regime [5], polaritons are continuously injected into the *pump* state and, above a pump strength threshold, undergo coherent stimulated scattering into the *signal* and *idler* states. Superfluidity has been tested through frictionless flow [2] by triggering a traveling signal with an additional pulsed probe laser. Moreover, metastability of quantum vortices and persistence of currents have been proven by using a pulsed Laguerre-Gauss beam [4]. Vorticity has been observed to be transferred into the OPO signal and to persist in absence of the driving rotating probe.

The polaritonic system is intrinsically non-equilibrium: Continuous pumping is needed to balance the fast polariton decay, of the order of picoseconds, and maintain a steady state regime. In strong contrast with equilibrium superfluids, which ground state is flowless, pump and decay lead to currents that carry polaritons from gain to loss dominated regions. As a result of the interplay between these currents and a confining potential, polaritons non-resonantly injected into a microcavity have been shown to become unstable to spontaneous formation of vortices [6, 7] and vortex lattices [8]. For resonant excitation, currents arise in the OPO regime due to the simultaneous presence of pump, signal and idler emitting at different momenta (see Fig. 1). In this Letter we identify a regime of the OPO, where remarkably, even in the absence of disorder or trapping potentials, the system undergoes spontaneous breaking of the system symmetry and becomes unstable towards the formation of a quantized vortex state with charge $m = \pm 1$. We show that these spontaneous stable vortex solutions are robust to

noise and to any other external perturbation, and thus should be experimentally observable. Spontaneous stable vortices differ from metastable ones, which can only be injected externally into an otherwise stable symmetric state, and which persistence is due to the OPO superfluid properties [4]. The metastable vortex is a possible but not unique stable configuration of the system. We find that shape and size of the metastable vortices are independent on the external probe. In addition, like in equilibrium superfluids, both stable and metastable vortices are characterised by a healing length which is determined by the parameters of the OPO system alone. Controlled creation of vortices in OPO has been recently achieved by a weak continuous probe [9]. Metastable vortices have been also recently discussed for non-resonantly pumped polariton condensates in Ref. [10].

Model We describe the OPO dynamics via Gross-Pitaevskii (GP) equations [11] for coupled cavity and exciton fields $\psi_{C,X}(\mathbf{r}, t)$ with pumping and decay ($\hbar = 1$):

$$i\partial_t \begin{pmatrix} \psi_X \\ \psi_C \end{pmatrix} = \begin{pmatrix} 0 \\ F_p + F_{pb} \end{pmatrix} + \begin{pmatrix} \omega_X - i\kappa_X + g_X|\psi_X|^2 & \Omega_R/2 \\ \Omega_R/2 & \omega_C - i\kappa_C \end{pmatrix} \begin{pmatrix} \psi_X \\ \psi_C \end{pmatrix}. \quad (1)$$

We neglect the exciton dispersion and assume a quadratic dispersion for photons, $\omega_C = \omega_C^0 - \frac{\nabla^2}{2m_C}$. The fields decay with rates $\kappa_{X,C}$ and Ω_R is the Rabi splitting. The cavity field is driven by a continuous wave pump,

$$F_p(\mathbf{r}, t) = \mathcal{F}_{f_p, \sigma_p}(r) e^{i(\mathbf{k}_p \cdot \mathbf{r} - \omega_p t)}, \quad (2)$$

where $\mathcal{F}_{f_p, \sigma_p}$ is either a Gaussian or a top-hat spatial profile with strength f_p and full width at half maximum (FWHM) σ_p . The exciton interaction strength g_X can be set to one by rescaling both fields $\psi_{X,C}$ and pump strength F_p by $\sqrt{\Omega_R/(2g_X)}$. For the simulations shown in this Letter $m_C = 2 \times 10^{-5} m_0$, the energy zero is fixed

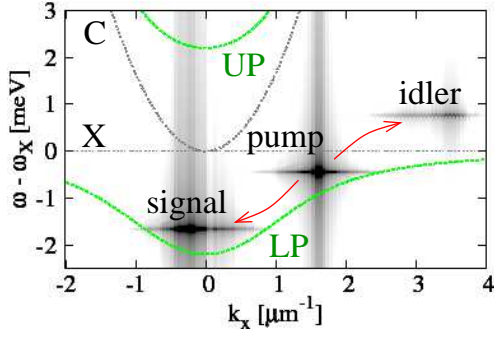


FIG. 1: (Color online) OPO spectrum for a top-hat pump of FWHM $\sigma_p = 70\mu\text{m}$ and intensity $f_p = 1.24f_p^{\text{th}}$, where f_p^{th} is the threshold strength for OPO. Polaritons injected resonantly at $(k_p, 0)$ and ω_p undergo coherent stimulated scattering into the signal and idler states, which are blue-shifted with respect to the bare lower polariton (LP) dispersion (green dotted line) because of interactions. Cavity photon (C) and exciton (X) dispersions are plotted as gray dotted lines.

to $\omega_X = \omega_C^0$ (case of zero detuning), $\Omega_R = 4.4\text{meV}$ and $\kappa_{X,C}$ are fixed so that to give a polariton lifetime of 3ps .

For homogeneous pumps, the conditions under which a stable OPO switches on can be found analytically by making use of the plane-wave approximation [12, 13]. However, for a finite size pump (2), one has to resort to a numerical analysis [11]. Here, we numerically solve Eq. (1) on a 2D grid by using both a 5th-order adaptive-step Runge-Kutta algorithm and the Crank-Nicholson method. Fixing the pump momentum $(k_p, 0)$ close to the LP inflection point, we find the pump strength threshold f_p^{th} for which signal and idler states get exponentially populated. The OPO signal spatial profile $|\psi_{C,X}^s|e^{i\phi_{C,X}^s}$ can be obtained by either filtering in a cone around the signal momentum at a given time or by filtering the time resolved spectrum in an interval around the signal energy (see Fig. 1). The photon component of the filtered OPO signal profile $|\psi_C^s|$ and its supercurrent $\nabla\phi_C^s$ are shown in the first left panel of Fig. 2. We only select OPO solutions which reach a steady state. Note that the pump direction $(k_p, 0)$ leaves the symmetry $y \mapsto -y$ intact. This symmetry, while allowing vortex-antivortex pairs, does not permit single vortices.

One can perform a dynamical stability analysis of the OPO by adding small fluctuations to the steady state mean-field: The existence of modes with positive imaginary part in the excitation spectrum indicates dynamical instability towards the growth of different modes. Equivalently, stability can be checked numerically by introducing a weak noise. In particular, we add white noise as a quick pulse to both modulus $|\psi_{X,C}(\mathbf{k}, t)|$ and phase $\phi_{X,C}(\mathbf{k}, t)$ of excitonic and photonic wavefunctions in momentum space. The noise added to the phase has amplitude 2π , and for the modulus we specify the noise

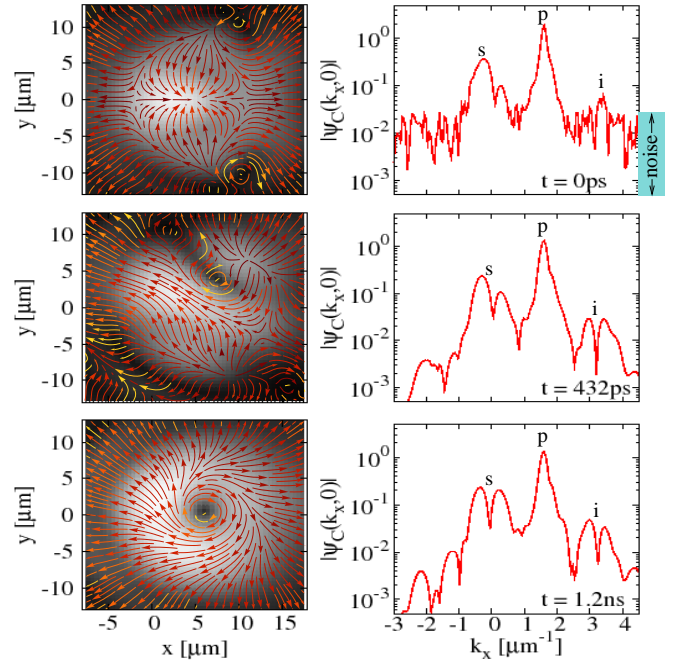


FIG. 2: (Color online) Filtered signal profile $|\psi_C^s(\mathbf{r}, t)|$ with supercurrents $\nabla\phi_C^s(\mathbf{r}, t)$ (left panels) and full momentum emission $|\psi_C(k_x, 0, t)|$ (right in arb. units) at three different times: $t = 0$ (first row), $t = 432\text{ps}$ (second) and 1.2ns (third). The strength of the $\sigma_p = 35\mu\text{m}$ top-hat pump is $f_p = 1.12f_p^{\text{th}}$. At $t = 0$ a pulsed weak random noise of strength 0.01 (see text) is added to the OPO steady state (first row) and at $t = 432\text{ps}$ a vortex, with $m = -1$, enters the signal and settles into a steady state. The noise strength only influences the time required for the vortex to appear.

strength in units of the maximum of the pump intensity in momentum space.

Stable vortex solutions Remarkably, we have singled out steady symmetric OPO states, as shown in the first row of Fig. 2, which are unstable towards the spontaneous formation of stable vortex solutions. Once the $y \mapsto -y$ symmetry is broken by the noise pulse of any strength, we have observed a vortex with quantised charge $m = \pm 1$ ($m = \mp 1$) entering and stabilising into the OPO signal (idler). In the case of Fig. 2 and the right panel of Fig. 3, the noise strength is 0.01 and 432ps after the noise pulse, a vortex with $m = -1$ ($m = +1$) enters the signal (idler) and stabilises. Different noise strengths do not affect the final steady state, but only the *transient* time the system needs to accommodate the vortex and reach the steady configuration. Note that parametric scattering constrains the phases of pump, signal and idler by $2\phi_p = \phi_s + \phi_i$. Therefore a vortex in the signal implies an antivortex in the idler and viceversa.

Further, we examine whether this vortex steady state is dynamically stable by applying an additional noise pulse. For weak noise, with a strength up to 0.1, the vortex is

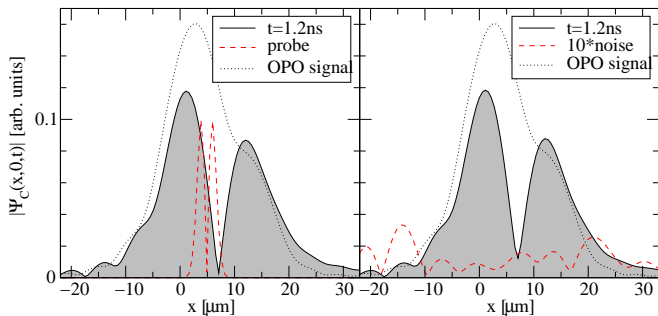


FIG. 3: (Color online) Steady state filtered signal profile (dotted line) $\psi_C^s(x,0,t)$ for $y \simeq 0$ before the arrival of either a vortex probe (3) with $\sigma_{pb} \simeq 1\mu\text{m}$ (left panel, red dashed line) or a noise pulse of strength 0.01 (right panel, red dashed line) — same OPO conditions as Fig. 2. After the arrival of any perturbation breaking the $y \mapsto -y$ symmetry, the same vortex with charge $m = \pm 1$ (solid shaded curve) stabilises into the signal.

stable and can only drift around a little before settling again into the same state. For strong noise, with strength 1 and above, the vortex gets washed away, but after a transient period, the very same state enters and stabilises again into the signal, with the possibility of flipping vorticity, as discussed later. Different noise strengths do not affect the final steady state, but only the transient time.

Alternatively, one can break the $y \mapsto -y$ symmetry by a weak pulsed vortex probe, and assess whether the stable steady state is in any way dependent on the external perturbation. As already shown in Refs. [4, 14], vortices with charge $m = \pm 1$ can be generated in the OPO signal and idler, by adding a Laguerre-Gauss pulsed probe:

$$F_{pb}(\mathbf{r}, t) = f_{pb} |\mathbf{r} - \mathbf{r}_{pb}| e^{-|\mathbf{r} - \mathbf{r}_{pb}|^2 / (2\sigma_{pb}^2)} e^{im\varphi} \times e^{i(\mathbf{k}_{pb} \cdot \mathbf{r} - \omega_{pb}t)} e^{-(t-t_{pb})^2 / (2\sigma_t^2)}, \quad (3)$$

where the probe momentum \mathbf{k}_{pb} and energy ω_{pb} are resonant with either the OPO signal or idler state. The phase φ winds from 0 to 2π around the vortex core \mathbf{r}_{pb} . Shortly after the arrival of the pulsed probe ($\sigma_t = 1\text{ps}$) there are two possible scenarios: either the vortex is imprinted into the signal and idler and drifts around, or no vortex gets transferred. However, the homogeneous OPO states which are unstable towards the spontaneous formation of stable vortices following a white noise pulse, exhibit the same instability following a vortex probe pulse (see left panel of Fig. 3). The steady state vortex is independent on both the probe intensity f_{pb} and size σ_{pb} , however the weaker the probe the longer the vortex takes to stabilise, between 30 and 400ps for our system parameters. The stable vortex following the Laguerre-Gauss probe is exactly the same as the one triggered by a weak white noise (see right panel of Fig. 3), indicating that the probe acts only as a symmetry breaking perturbation.

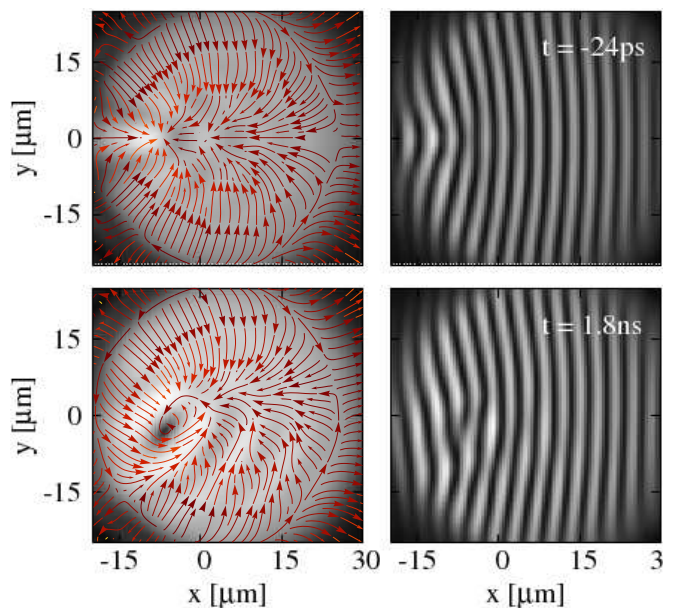


FIG. 4: (Color online) Generation of an $m = +1$ metastable vortex solution into the OPO signal ($f_p = 1.24f_p^{\text{th}}$ and $\sigma_p = 70\mu\text{m}$). First row: OPO filtered signal spatial profile together with currents (left) and interference fringes (right) are plotted at $t = -24\text{ps}$ before the arrival of either a strong enough vortex probe (3) or a strong enough noise pulse. The metastable vortex lasts for as long as our simulation (last row, $t = 1.8\text{ns}$) and requires a threshold in the intensity of the perturbation breaking the $y \mapsto -y$ symmetry. The vortex appears in the interference fringes as a fork-like dislocation.

We can therefore infer that there are OPO conditions, as the one of Fig. 2, where the $y \mapsto -y$ symmetric solution is dynamically unstable, and any symmetry breaking perturbation allows the signal and idler to relax into a stable steady state carrying a vortex with charge ± 1 . This suggests that such a vortex is the genuine unique OPO stable state, which however cannot be accessed without breaking the $y \mapsto -y$ symmetry. Instability of the uniform state to spontaneous pattern (e.g., vortex) formation is a typical feature of systems driven away from equilibrium [15]. Similarly we find conditions for which the uniform OPO solution is unstable to spontaneous formation of a quantised vortex.

The system symmetry can also be broken by spatial disorder. Indeed, as for non-resonantly pumped polaritons [6], we have found in our OPO simulations spontaneous stable vortices forming in a disordered landscape.

Metastability In addition to stable vortices, we have found OPO conditions supporting metastable vortex solutions. In this case, the symmetric OPO steady state is dynamically stable, but, because of its superfluid properties, can support persistent metastable currents injected externally. Metastable solutions can be equally induced by either a vortex probe (3) or a noise pulse. However,

differently from the stable case, such a solutions require a threshold in the perturbation breaking the system symmetry. One example is shown in Fig. 4: the steady state shown in the second row can be triggered by adding a white noise pulse to the symmetric OPO steady state (first row of Fig. 4) only for noise strengths larger than 0.1. For weaker noises, the OPO signal is slightly perturbed and rapidly goes back to its steady state vortexless configuration. Alternatively, a vortex probe (3) can also be applied. For example, for a probe vortex with $\mathbf{r}_{pb} \simeq (-6, -5)\mu\text{m}$, $\sigma_{pb} = 4.5\mu\text{m}$, which is resonant with the OPO signal momentum and frequency, a probe intensity $f_{pb} \geq 0.45f_p$ is required in order to generate the steady state vortex shown in the last row of the figure. Right panels of Fig. 4 show the interference fringes between signal and pump state, obtained by considering the full emission in space $|\psi_C(\mathbf{r}, t)|$. A vortex corresponds to a fork-like dislocation in the interferences.

The spatial position of both stable and metastable steady state vortices is close to the position where the OPO signal has the currents pointing inwards (see Figs. 2 and 4). We find stable vortices appearing quite close to the pump threshold. At higher powers, the OPO tends to switch off in the middle of the excitation spot and the system tends not to reach a steady state. Finally, we checked that $m = \pm 1$ ($m = \mp 1$) vortex solutions can appear only into the OPO signal (idler). A vortex probe pulse of any charge m injected resonantly to the pump momentum and energy gets immediately transferred to an $m = \pm 1$ ($m = \mp 1$) vortex in the signal (idler), leaving the pump vortexless. The stability of signal $m > 1$ vortices is outside the scope of this work [16].

Conservation of charge When generated by a noise pulse, stable and metastable vortices have equal probability to be triggered with either charge ± 1 . Similarly, when vortices are triggered via a vortex probe, their vorticity can flip during the transient period. Often, the flipping is caused by the spontaneous appearance of two antivortices at the edge of the signal, one recombining with the triggered vortex. Topological charge inversion has been already predicted to occur in confined atomic Bose-Einstein condensates at intermediate interactions strengths [17]: In the presence of an asymmetry, breaking rotation invariance, vorticity is not a conserved quantity.

Healing length An approximate analytical expression for the vortex healing length can be derived for homogeneous pumping, assuming that only signal and idler carry opposite angular momentum m ,

$$\psi^{s,i}(\mathbf{r}) = \sqrt{n_{s,i}} e^{i\mathbf{k}_{s,i} \cdot \mathbf{r}} e^{\pm im\varphi} \Psi^{s,i}(r),$$

while the pump remains in a plane-wave state, $\psi^p(\mathbf{r}) = \sqrt{n_p} e^{i\mathbf{k}_p \cdot \mathbf{r}}$, as supported by our numerical analysis. For pump powers close to OPO threshold, it can be shown that signal and idler steady state spatial profiles are locked together and satisfy the following complex GP

equation

$$\left[-\frac{1}{2m_C} \left(\frac{d^2}{dr^2} + \frac{1}{r} \frac{d}{dr} - \frac{m^2}{r^2} \right) + \alpha (|\Psi^s|^2 - 1) \right] \Psi^s = 0,$$

where $|\alpha| \simeq g_X \sqrt{n_s n_i}$. Keeping aside that α is a complex parameter, this equation describes a vortex profile [18] with healing length

$$\xi = (2m_C g_X \sqrt{n_s n_i})^{-1/2}. \quad (4)$$

This expression is similar to the one of an equilibrium superfluid, with the condensate density replaced by the square root of the product of the signal and idler densities. Further above threshold, the signal and idler profiles are no longer locked together, and they start to develop different radii. In both the simulations of Figs. 3 and 4, we find $\xi \simeq 4\mu\text{m}$, compatible with the estimate (4). Recently, the controlled creation of OPO vortices by a weak continuous probe [9] has allowed to experimentally test the validity of Eq. (4).

To conclude, we have shown that close to the OPO threshold, the polariton superfluid can spontaneously break the $y \mapsto -y$ system symmetry and, even in absence of driving rotation, trapping, or disorder potential, can be unstable towards the creation of a quantised vortex state of charge ± 1 . While the OPO symmetric state is generally stable, metastable vortices can be injected by a strong enough external probe. The size of both types of vortices is given by a healing length, which, close to threshold, is analogous to the one of equilibrium superfluids. Long lived metastable vortices have been experimentally realised in Ref. [4], providing an evidence for existence of persistent currents in this system. Since the parameters of our simulations are close to those of current semiconductor microcavities, the existence of stable spontaneous vortices in OPO should also be within experimental reach. Moreover, these stable vortex states are very robust to noise. Thus, apart from being yet another example of exotic behaviour in polariton superfluids, they carry potential for applications in, e.g., quantum information.

We are grateful to J.J. García-Ripoll, D. Sanvitto, J. Keeling, N.G. Berloff, and L. Viña for stimulating discussions. F.M.M. acknowledges financial support from the programs Ramón y Cajal and INTELBIOMAT (ESF). This work is in part supported by the Spanish MEC (MAT2008-01555, QOIT-CSD2006-00019) and CAM (S-2009/ESP-1503). We thank TCM group (Cavendish Laboratory, Cambridge) for the use of computer resources.

* also at London Centre for Nanotechnology, UK

- [1] P. G. Savvidis, et al., Phys. Rev. Lett. **84**, 1547 (2000).
- [2] A. Amo, et al., Nature **457**, 291 (2009).
- [3] A. Amo, et al., Nat. Phys. **5**, 805 (2009).

- [4] D. Sanvitto, et al. (2009), arXiv:0907.2371.
- [5] R. M. Stevenson, et al., Phys. Rev. Lett. **85**, 3680 (2000).
- [6] K. G. Lagoudakis, et al., Nature Physics **4**, 706 (2008).
- [7] G. Nardin, et al., arXiv:1001.0846.
- [8] J. Keeling and N. G. Berloff, Phys. Rev. Lett. **100**, 250401 (2008).
- [9] D. N. Krizhanovskii, et al., Phys. Rev. Lett., to appear.
- [10] M. Wouters and V. Savona (2009), cond-mat/0904.2966.
- [11] D. M. Whittaker, phys. stat. sol. (c) **2**, 733 (2005).
- [12] D. M. Whittaker, Phys. Rev. B **71**, 115301 (2005).
- [13] C. Ciuti, P. Schwendimann, and A. Quattropani, Semi-cond. Sci. Technol. **18**, S279 (2003).
- [14] D. M. Whittaker, Superlatt. and Microstruct. **41**, 297 (2007).
- [15] M. C. Cross and P. C. Hohenberg, Rev. Mod. Phys. **65**, 851 (1993).
- [16] M. H. Szymańska and F. M. Marchetti, in preparation.
- [17] J. J. García-Ripoll, G. Molina-Terriza, V. M. Pérez-García, and L. Torner, Phys. Rev. Lett. **87**, 140403 (2001).
- [18] L. P. Pitaevskii and S. Stringari, *Bose-Einstein Condensation* (Clarendon Press, Oxford, 2003).